

# Using the Imidazole and Benzimidazole as Corrosion Inhibitor of UNS S31803 Duplex Stainless Steel

Roberta Rossi Moreira, Thiago Freitas Soares, Leonardo Cabral Gontijo, Eustáquio V. Ribeiro de Castro, Josimar Ribeiro

**Abstract**— The behavior of corrosion and corrosion inhibition of UNS S31803 duplex stainless steel (DSS) were studied in sodium chloride solution (3.0 wt. %), in the absence and presence of benzimidazole and imidazole corrosion inhibitors. The chemical and morphological characterization of steels were performed using the techniques such as optical emission spectrometry, X-ray diffraction (XRD), optical microscopy, scanning electron microscopy (SEM) and energy dispersive X-ray (EDX). Electrochemical analysis were performed through the techniques of potentiodynamic polarization and electrochemical impedance spectroscopy. XRD analysis showed that the UNS S31803 DSS displayed austenite and ferrite phases. Additionally, metallographic and SEM and EDX analysis allowed to identify certain regions and elements present in the steel which provide corrosion occurring, such as inclusions. The inhibitors were tested at different concentrations (25 ppm, 50 ppm, 100 ppm, 500 ppm and 1000 ppm) for the three steel through the polarization curves and electrochemical impedance, and it was found that all concentrations showed an increase in corrosion resistance. Polarization curves analysis showed that the benzimidazole provided to UNS S31803 DSS, inhibition efficiencies of about 75 %. While imidazole showed an efficiency of about 86 %. The electrochemical impedance results showed that the inhibition efficiencies was approximately 71 % for benzimidazole and of about 85 % for the imidazole. In all electrochemical analysis imidazole proved to be the better inhibitor for the DSS investigated.

**Index Terms**— Benzimidazole, Duplex Stainless Steel, EIS, Imidazole.

## I. INTRODUCTION

Duplex stainless steels (DSS) may be defined as a family of steels having a two phase ferritic-austenitic microstructure, the components of which are both stainless, i.e. contain more

**Manuscript received March 09, 2016**

**Roberta Rossi Moreira**, Departamento de Química do Centro de Ciências Exatas/UFES, Av. Fernando Ferrari, 514, 29075-910, Vitória/ES, Brazil

**Thiago Freitas Soares**, Departamento de Química do Centro de Ciências Exatas/UFES, Av. Fernando Ferrari, 514, 29075-910, Vitória/ES, Brazil

**Leonardo Cabral Gontijo**, Instituto Federal de Educação, Ciência e Tecnologia do Espírito Santo, Av. Vitória

**Eustáquio V. Ribeiro de Castro**, Departamento de Química do Centro de Ciências Exatas/UFES, Av. Fernando Ferrari, 514, 29075-910, Vitória/ES, Brazil

**Josimar Ribeiro**, Departamento de Química do Centro de Ciências Exatas/UFES, Av. Fernando Ferrari, 514, 29075-910, Vitória/ES, Brazil

than 13 % Cr wt.% [1]. Duplex ferritic-austenitic steels have been available for some time and offer higher strength, better stress corrosion cracking resistance and, in some instances, superior pitting resistance to 316L austenitic alloys [2]. To obtain these properties, an appropriate combination of chemical composition and the absence of undesirable intermetallic phases in the microstructure is required [3].

To preserve the integrity of metallic materials, some measures to inhibit or prevent corrosion in many aggressive media are cited in the literature [4]. Organic inhibitors that exhibit one or more polar functions (such as N, O and S) and heterocyclic compounds with polar groups and  $\pi$  electrons have been quite effective in corrosion protection [5]. This inhibition efficiency is usually attributed to the specific interactions that occur between functional groups and heteroatoms with the metal surface due to their lone pair electrons and the influence on the change of corrosion potential [6].

Our goal was to study the behavior of corrosion and corrosion inhibition of UNS S31803 duplex stainless steel (DSS) in sodium chloride solution (3.0 wt. %), in the absence and presence of benzimidazole and imidazole corrosion inhibitors.

## II. EXPERIMENTAL SECTION

### A. Samples

The samples used in this study were UNS S31803 duplex stainless steel (DSS) with the chemical compositions listed in Table 1. The samples were prepared in two different ways. For morphological analysis, the samples were prepared in a square shape, with dimensions of 1.0 cm x 1.0 cm. For the electrochemical investigations, the samples were L-shaped, with dimensions of 3.0 cm x 1.0 cm. Each sample was prepared to leave an area of 1.0 cm<sup>2</sup> to test, which was isolated with the aid of an epoxy resin (Araldite®).

Before performing each analysis, the samples were subjected to cleaning and polishing of the surface using sandpaper of several different particle sizes in water, respectively, in the following order: 220, 320, 400, 600 and 1200 mesh. The polishing was finished with 0.3  $\mu$ m alumina to obtain a uniform surface. At each change of sanding, the sample was rotated 90°. The specimens were then washed with distilled water, degreased with acetone and dried with a hot air blast. Before and after every analysis, the samples were stored in argon to prevent contamination by contact with the external environment.

### B. XRD, LIPS, EDS and SEM

The XRD analyses were carried out on a Bruker model D8 Discover diffractometer operating with Cu K $\alpha$  radiation ( $\lambda = 1.5406 \text{ \AA}$ ) generated at 40 kV and 40 mA;  $2\theta$  was scanned from  $20^\circ$  to  $100^\circ$  at a scan rate of  $2^\circ \text{ min}^{-1}$ . The EVA V3.1 software was used to process the XRD data.

Laser-induced plasma emission spectroscopy (LIPS) using a Foundry-Master Pro spectrometer of the Shimadzu Corporation equipped with an Echelle optics and Kodak KAF 1001 ICCD detector allowed us to estimate the chemical composition of the alloys.

Metallographic analysis was performed to reveal the microstructure of steels. A chemical attack was performed on the sample of UNS S31803 duplex stainless steel with 1:3 HNO<sub>3</sub>:HCl solution for 20 seconds to reveal the structure of the austenite grains and the presence of carbides. Microstructural characterization was performed using a Nikon Eclipse 200 MA optical microscope at 1000x magnification with polarized light. A Shimadzu SS550 scanning electron microscope (SEM) coupled to an SEDX model analyzer was used to investigate the corrosion morphology. The EDS results were obtained from the matrix interference, atomic number, absorbance, and fluorescence (ZAF correction) data.

### C. Electrochemical investigations

Electrochemical measurements were performed using a 100 mL capacity electrochemical cell with three electrodes. The reference electrode was Ag/AgCl(KCl, 3.0 mol L<sup>-1</sup>), the counter electrode was carbon with dimensions of 2.1 cm x 0.5 cm x 1.8 cm, and the working electrode was of UNS S31803 duplex stainless steel. For electrochemical tests, a potentiostat/galvanostat AUTOLAB PGSTAT model 302N and GPES software were used. The corrosion tests were performed in duplicate using reagents to prepare solutions and analytical grade deionizer water with a conductivity of 23.07 mS cm<sup>-1</sup> at 25°C from a deionizer trademark of Union analysis. The temperature was monitored and remained at  $24 \pm 1.0^\circ\text{C}$ . The corrosive media used in the tests were composed of sodium chloride at 3.0 wt. % using PA-Impex reagent ACS in the presence or absence of benzimidazole (Sigma-Aldrich, 98%) and/or imidazole (Sigma-Aldrich, 98%). Imidazole and benzimidazole were employed as corrosion inhibitors at different concentrations: 25, 50, 100, 500 and 1000 ppm. For Tafel polarization measurements, the potential was varied by  $\pm 250 \text{ mV}$  from the open circuit potential ( $E_{\text{ocp}}$ ) at a scan rate of  $0.5 \text{ mV s}^{-1}$ .  $E_{\text{ocp}}$  was obtained by measuring electrochemical noise and was measured until the system came into balance for a period of 4000 seconds.

## III. RESULTS SECTION

### A. Structural characterization

When Figure 1 shows the XRD pattern of the UNS S31803 duplex stainless steel. It can be see diffraction peaks at  $2\theta$ :  $43.62^\circ$ ,  $50.81^\circ$  and  $74.71^\circ$ , which can be associated to single-phase austenite ( $\gamma$ -Fe), cubic crystal structure of face-centered, whose lattice parameter value is  $3.6070 \pm 0.0033 \text{ \AA}$  and volume is  $46.93 \pm 0.13 \text{ \AA}^3$ , due to the present of planes (111), (200) and (202) as seen in PDF-90-08469 [7]. It is also observed that the diffraction peak at the angle  $50.81^\circ$  may refer to the chrome phase (Cr), as PDF-01-088-2323 [7].

In addition to these peaks were noted at angles others  $44.71^\circ$ ,  $65.08^\circ$  and  $82.41^\circ$  that can be associated with the ferrite phase ( $\alpha$ -Fe), which exhibits cubic body-centered crystal structure, whose lattice parameter value is  $2.8797 \pm 0.0011 \text{ \AA}$  and volume is  $23.88 \pm 0.03 \text{ \AA}^3$ , with diffraction planes (110), (200) and (211) as shown in PDF-06-0696 [7]. According to the analysis results, it is observed that there is this steel a mixed crystal structure composed of the two phases, austenite and ferrite, apparently being present in proportions, as it turns the amounts and intensities of the peaks shown in the diffraction pattern this characteristic X-ray present in the duplex steels is responsible for conferring to them an attractive combination of mechanical properties and corrosion resistance [8].

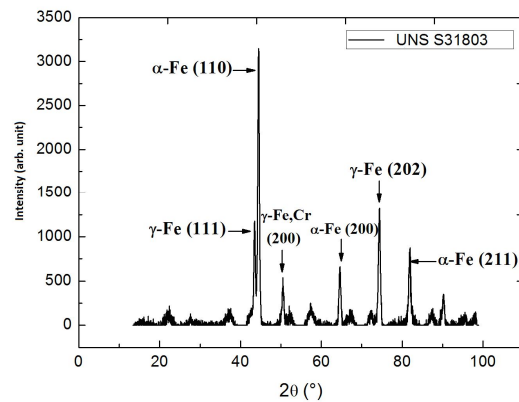


Fig. 1. XRD pattern of UNS S31803 duplex stainless steel.

Table 1. Chemical composition of the studied UNS S31803 (wt. %).

C	Mn	Si	Cr	Mo	P	S	Ni
0.0469	1.41	0.368	22.3	3.20	0.011	<0.0007	5.66

Metallographic image of the UNS S31803 duplex stainless steel is shown in Figure 2, which shows the microstructure and grain boundary phases present in the steel. According to the obtained image the attack carried out revealed the ferrite phase grain boundaries leaving unattacked austenite phase. As can be seen DSS has a mixed microstructure having approximately the same proportion of the two phases present, which offers greater resistance to localized corrosion, particularly of the type pitting and corrosion crack [8].

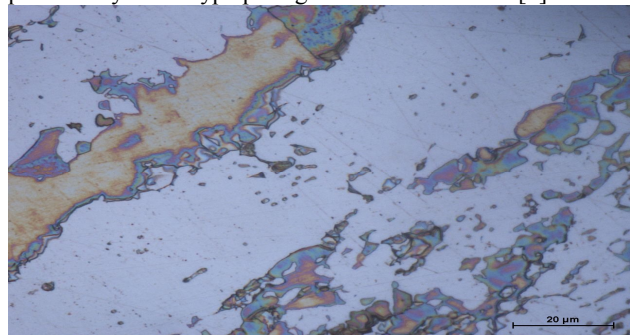
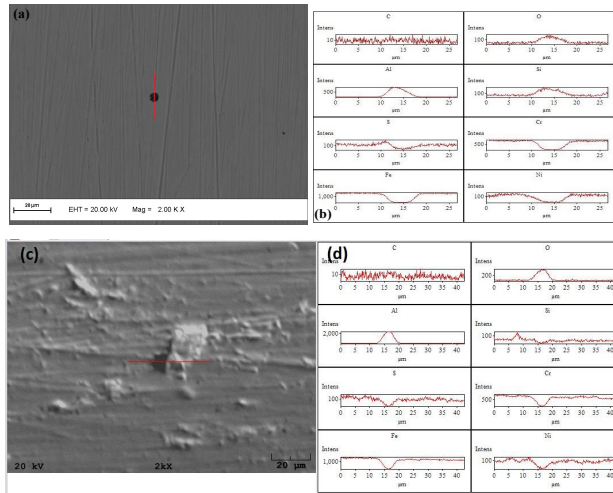


Fig. 2. Metallographic image of UNS S31803 duplex stainless steel with 1000x magnification.



**Fig. 3.** SEM images of UNS S31803 duplex stainless steel with 2000x magnification. (a) and (b) before corrosion process. (c) and (d) after corrosion process.

From the SEM-EDS images obtained of the UNS S31803 duplex stainless steel before corrosion process (see Figures 3a and 3b), there is the presence of nonmetallic inclusion with a globular shape and of smaller diameter compared to the inclusion found in stainless steel AISI 316 [9, 10]. The EDS analysis shows the elemental composition of the inclusion found in the sample. From this analysis it was observed that the inclusion is comprised predominantly of aluminum, silicon and oxygen indicating that can be treated Al and Si oxides, and observing a small upward peak corresponding sulfur.

Elements such as oxygen, sulfur, nitrogen, phosphorous, chlorine, sodium, and potassium are the key from the steel making process and are responsible for generating negative effects on the properties of steels, causing brittleness and poor corrosion resistance. In order to reduce the amount of oxygen and sulfur in the alloy Al and Si elements, for example, are added to the melt shop to perform the process of deoxidizing the molten metal, that due to the strong reactivity of these elements to oxygen forming their oxides.

After corrosion process, it was observed that the DSS surface was modified with the appearance of roughness. Such corrosion is called blistering occurs by hydrogen and because of penetration of atomic hydrogen in the metallic material, through discontinuities such as inclusions and voids. Discontinuities in the atomic hydrogen is transformed into molecular hydrogen, which puts pressure causing the formation of blistering.

### B. Electrochemical characterization

Figures 4 and 5 reveals the Tafel curves obtained for the UNS S31803 DSS in 3.0 wt.% NaCl solutions at  $24 \pm 1.0$  °C in the presence of different benzimidazole and imidazole concentrations (from 5 mg/L to 1000 mg/L), respectively. It can be seen that in the presence of benzimidazole or of imidazole as an inhibitor, it occurred displacement of potential corrosion ( $E_{corr}$ ) to more positive potentials, compared with the curves in the absence of inhibitors.

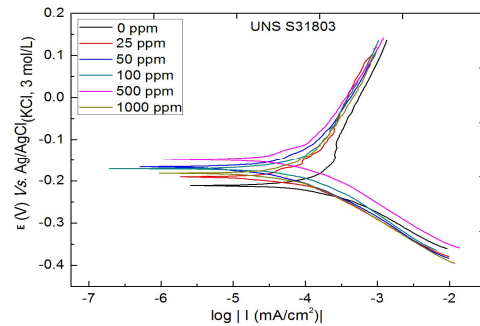


**Fig. 4.** Tafel plots of the UNS S31803 DSS in the presence of 3.0 wt.% solution of chloride ions. Temperature =  $24 \pm 1.0$  °C; scan rate of  $0.5 \text{ mV s}^{-1}$  in different benzimidazole concentrations.

We have investigated the EIS behavior of the UNS S31803 DSS in 3.0 wt.% solution of chloride ions at 24 in the presence and absence of the inhibitor (benzimidazole and/or imidazole). Figure 6 show the Nyquist diagram (Fig. 6a and 6c) and Bode plots (Fig. 6b and 6d) for the DSS obtained at corrosion potential in the presence of benzimidazole and imidazole inhibitors. In the all frequency domain, the DSS give a deformed semicircle, attributed to the metal/solution interface. The same behavior was observed for others stainless steel studied using EIS [10]. Tables 2 and 3 summarizes the  $R_p$ -values obtained by EIS as well as others parameters simulated in this investigation.

It is seen in the Figure 6b that there was a change in phase angles at low frequency, in the presence of benzimidazole, but not very pronounced, with the  $72.5^\circ$ ,  $72.6^\circ$ ,  $75.5^\circ$ ,  $75.4^\circ$ ,  $74.2^\circ$  and  $74.3^\circ$  obtained in the absence and presence of  $25 \text{ mg L}^{-1}$ ,  $50 \text{ mg L}^{-1}$ ,  $100 \text{ mg L}^{-1}$ ,  $500 \text{ mg L}^{-1}$  and  $1000 \text{ mg L}^{-1}$  of benzimidazole, respectively. Moreover, it appears that there was a widening of frequencies in the presence of the benzimidazole. However, as noted, the maximum phase angle and further increase of the frequency has been obtained at a concentration of  $50 \text{ mg L}^{-1}$ . This suggests that there was the formation of protective film on the DSS surface, protecting it from the corrosive medium. The better  $R_p$ -value observed for the UNS S31803 DSS was at a concentration of  $50 \text{ mg L}^{-1}$  ( $143.9 \text{ k}\Omega \text{ cm}^2$ ). By calculating the inhibition efficiency for this concentration it was obtained a value of 71.3%, very close to the efficiency found by Tafel analysis (75.3%).

However, when we using the imidazole as inhibitor it was observed that the  $100 \text{ mg L}^{-1}$  was the better concentration for this inhibitor with  $R_p$ -value of  $284.3 \text{ k}\Omega \text{ cm}^2$ , with 85.5% of inhibition efficiency, very close to the value found by analysis of the curves Tafel which was 86.1%



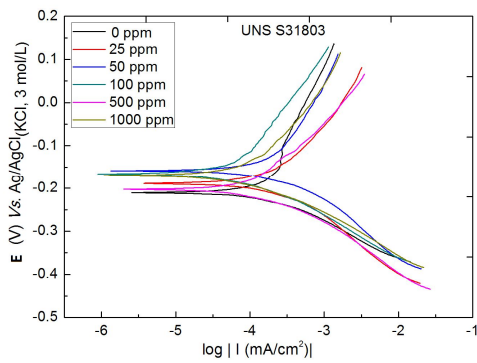


**Fig. 5.** Tafel plots of the UNS S31803 DSS in the presence of 3.0 wt.% solution of chloride ions. Temperature = 24 ± 1.0 °C; scan rate of 0.5 mV s<sup>-1</sup> in different imidazole concentrations.

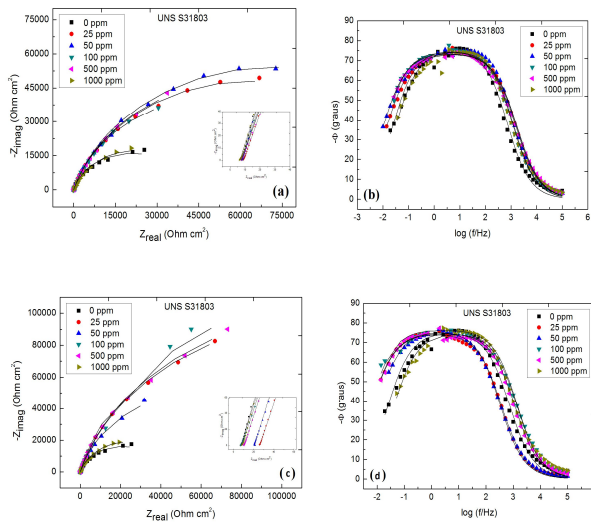


**Fig. 6.** (a and c) Nyquist diagram and (b and d) Bode plot of the UNS S31803 DSS in the presence of 3.0 wt.% solution of chloride ions. Temperature = 24 ± 1.0 °C. (a and b) benzimidazole and (c and d) imidazole.

**Table 2.** EIS parameters obtained by data simulations of the UNS S31803 DSS in the presence of 3.0 wt.% solution of chloride ions. Temperature = 24 ± 1.0 °C in different benzimidazole concentrations\*.

inhibitor mg L <sup>-1</sup>	R <sub>s</sub> Ω cm <sup>2</sup>	R <sub>p</sub> kΩcm <sup>2</sup>	EFC/ Y <sub>0</sub>	EFC/n	C <sub>dc</sub> (μFcm <sup>-2</sup> )	n (%)
0	7.23	41.25	113.7	0.8427	97.18	-
25	8.89	128.14	56.34	0.8197	67.81	71.3
50	7.79	143.88	65.52	0.8223	60.68	61.76
100	7.65	107.86	77.71	0.8338	79.53	68.4
500	7.54	130.86	71.13	0.8221	72.91	6.46
1000	6.49	44.09	85.18	0.8378	87.13	

\*Chi-Square observed ranged from 10<sup>-3</sup> to 10<sup>-4</sup>.  
\*The error for R<sub>p</sub>-values was of 8.5% maximum.

**Table 3.** EIS parameters obtained by data simulations of the UNS S31803 DSS in the presence of 3.0 wt.% solution of chloride ions. Temperature = 24 ± 1.0 °C in different imidazole concentrations\*.

inhibitor mg L <sup>-1</sup>	R <sub>s</sub> Ω cm <sup>2</sup>	R <sub>p</sub> kΩ cm <sup>2</sup>	EFC/Y <sub>0</sub>	EFC/n	C <sub>dc</sub> μF cm <sup>-2</sup>	n (%)
0	7.23	41.25	113.74	0.8427	97.18	-
25	25.86	249.12	60.07	0.8332	61.48	83.44
50	20.68	132.59	74.03	0.8484	75.61	68.89
100	7.36	284.31	59.91	0.8529	59.91	85.49
500	10.25	260.58	58.91	0.8355	60.27	84.17
1000	8.22	49.36	62.02	0.8372	63.44	16.44

\*Chi-Square observed ranged from 10<sup>-3</sup> to 10<sup>-4</sup>.  
\*The error for R<sub>p</sub>-values was of 10 % maximum.

CONCLUSION

This paper showed the investigation of the UNS S31803 duplex stainless steel using different techniques in 3.0 wt.% solution of chloride ions in the presence and absence of benzimidazole and imidazole as corrosion inhibitors. The inhibition efficiency evaluated in this work attested that all the concentrations increase the corrosion potential. Tafel and EIS results analysis proved that the imidazole was the better inhibitor for the DSS investigated.

ACKNOWLEDGMENT

The authors thank FAPES, CAPES, CNPq, UFES, PETROBRAS, IFES, LPT-UFES TRICORRMAT-UFES.

REFERENCES

- [1] J.-O Nilsson, "Overview: Super duplex stainless steels", *Materials Science and Technology*, vol. 8, no. 29, pp.685-700, 1992.
- [2] T. J. Glover, "Application of stainless steels in chemical plant corrosive environments", *Anti-Corrosion Methods and Materials*, vol. 29, no. 3, pp. 11-12, 1982.
- [3] K. H. Lo, C. H. Shek, J. K. L. Lai, "Recent developments in stainless", *Materials Science Engineering*. vol. R 65, pp. 39-104, 2009.
- [4] D.A. Shifler, "Understanding material interactions in marine environments to promote extended structural life", *Corrosion Science*, vol. 47, pp. 2335-2352, 2005.
- [5] A.M. Fekry, and M.A. Ameer, "Corrosion inhibition of mild steel in acidic media using newly synthesized heterocyclic organic molecules" *International Journal of Hydrogen Energy*, vol. 35, pp. 7641-7651, 2010.
- [6] E. Lunarska and O. Chernyayeva, "Effect of corrosion inhibitors on hydrogen uptake by Al from NaOH solution", *International Journal of Hydrogen Energy*, vol. 31, pp. 285-293, 2006.
- [7] Powder Diffraction File: 01-088-2323, 90-08469, 06-0696. Joint Committee on Powder Diffraction Standards, International Center for Diffraction Data, vol. PDF-2, Pennsylvania, USA, 2011.
- [8] TAN, H.; JIANG, Y. M.; DENG, B.; SUN, T.; XU, J.; LI, J., "Effect of annealing temperature on the pitting corrosion resistance of super duplex stainless UNS S32750" *Mater. Charact.*, vol. 60, pp. 1049-1054, 2009.
- [9] R. R. Moreira, T. F. Soares, J. Ribeiro, "Electrochemical investigation of corrosion on AISI 316 stainless steel and AISI 1010 carbon steel: Study of the behaviour of imidazole and benzimidazole as corrosion inhibitors" *Advances in Chemical Engineering and Science*, vol. 4, pp. 503-514, 2014.
- [10] T. F. Soares, R. R. Moreira, A. R. de Andrade, J. Ribeiro, "Corrosion behavior of AISI 304 and AISI 430 stainless steels in presence of benzimidazole inhibitor" *International Journal of Engineering Innovation & Research*, vol. 4, pp. 220-226, 2015.



**Roberta Rossi Moreira** has a degree in Chemistry by the Federal Institute of the Espírito Santo (IFES), Postgraduate in Industrial Chemistry (FAESA) and Master in Chemistry from the Federal University of Espírito Santo, 2014 (UFES).



**Thiago Freitas Soares** has a degree in Chemistry from the Federal University of Espírito Santo (2012), degree in Chemical Engineering from the Central East College (2014) and master's degree in chemistry from the Federal University of Espírito Santo (2014). Has experience in Chemistry.



**Leonardo Cabral Gontijo** is Titular professor of the Federal Institute of the Espírito Santo. Graduated in Full Degree in Physics from the Federal University of Espírito Santo (1983), MSc in Physics from the Federal University of Espírito Santo (1996) and PhD in Materials Science and Engineering from the Federal University of São Carlos (2002). Has experience in the area of Materials and Metallurgical Engineering, with emphasis on Surface Treatments, acting on the following subjects: plasma, plasma nitriding, corrosion, characterization and stainless steel.



**Eustáquio V. Ribeiro de Castro** is graduated in Full Degree in Chemistry from the Federal University of Uberlândia (1985), MSc in Chemistry from the Federal University of Minas Gerais (1989) and PhD in Chemistry from the São Paulo University (1996). He has experience in Chemistry, focusing on Theoretical Chemistry, acting on the following subjects: petroleum, generator coordinate Hartree-Fock method, gaussian basis sets.



**Josimar Ribeiro** is associate professor of Federal University of the Espírito Santo. He obtained his BS degree in 1999 from University of São Paulo/Faculdade de Filosofia, Ciências e Letras de Ribeirão Preto, MS degree in 2002, and his doctorate in 2006 from University of São Paulo/Faculdade de Filosofia, Ciências e Letras de Ribeirão Preto. He was awarded the Diploma of Merit and Lavoisier Prize for being the best student of BS in Chemistry awarded by the CRQ-IV, Regional Council of Chemistry-IV region (1996-1999). Conducted the first post-doctoral fellow at Université de Poitiers - France (2007) working with catalysis

for fuel Cell (CAPES). He is author of 24 scientific publications, six books and two chapters in books.